Journal of Biomechanics 85 (2019) 126–133

Contents lists available at ScienceDirect

Journal of Biomechanics

journal homepage: www.elsevier.com/locate/jbiomech
www.JBiomech.com

Including surrounding tissue improves ultrasound-based 3D mechanical characterization of abdominal aortic aneurysms ☆

Niels J. Petterson [a,*], Emiel M.J. van Disseldorp [a,b], Marc R.H.M. van Sambeek [a,b], Frans N. van de Vosse [a], Richard G.P. Lopata [a]

[a] Cardiovascular Biomechanics Group, Department of Biomedical Engineering, Eindhoven University of Technology, P.O. Box 513, 5600 MB Eindhoven, the Netherlands
[b] Department of Surgery, Catharina Hospital Eindhoven, P.O. Box 1350, 5602 ZA Eindhoven, the Netherlands

ARTICLE INFO

Article history:
Accepted 10 January 2019

Keywords:
Abdominal aortic aneurysm
Wall stress
Ultrasound
Speckle tracking
Arterial stiffness

ABSTRACT

Objectives: In this study the influence of surrounding tissues including the presence of the spine on wall stress analysis and mechanical characterization of abdominal aortic aneurysms using ultrasound imaging has been investigated.
Methods: Geometries of 7 AAA patients and 11 healthy volunteers were acquired using 3-D ultrasound and converted to finite element based models. Model complexity of externally unsupported (aorta-only) models was complemented with inclusion of both soft tissue around the aorta and a spine support dorsal to the aorta. Computed 3-D motion of the aortic wall was verified by means of ultrasound speckle tracking. Resulting stress, strain, and estimated shear moduli were analyzed to quantify the effect of adding surrounding material supports.
Results: An improved agreement was shown between the ultrasound measurements and the finite element tissue and spine models compared to the aorta-only models. Peak and 99-percentile Von Mises stress showed an overall decrease of 23–30%, while estimated shear modulus decreased with 12–20% after addition of the soft tissue. Shear strains in the aortic wall were higher in areas close to the spine compared to the anterior region.
Conclusions: Improving model complexity with surrounding tissue and spine showed a homogenization of wall stresses, reduction in homogeneity of shear strain at the posterior side of the AAA, and a decrease in estimated aortic wall shear modulus. Future research will focus on the importance of a patient-specific spine geometry and location.

1. Introduction

Current clinical guidelines for abdominal aortic aneurysm (AAA) repair use the maximum anterior-posterior diameter as criterion to assess the risk of rupture (Moll et al., 2011). In general, when the diameter exceeds 5.5 cm for men and 5.2 cm for women, or the growth rate surpasses 1 cm per year, the risk of rupture is deemed higher than the risks involved with aortic aneurysm repair (The UK Small Aneurysm Trial Participants, 1998). These guidelines are based on large population studies but are not tailored to predicting the rupture risk for the individual patient (Nicholls et al., 1998). As a consequence, ongoing research focuses on improving the patient-specific rupture risk assessment to prevent premature rupture.

Multiple strategies to determine the personalized rupture risk have been proposed, mainly focusing on the geometry and biomechanics of the vessel wall (Erhart et al., 2015; Fillinger et al., 2003; Gasser, 2016; Raghavan and Vorp, 2000). Wall stress analysis has been proposed, and many groups have investigated the use of image-based, discretized, (semi)patient-specific geometries determined with computed tomography (CT) (Indrakusuma et al., 2016), magnetic resonance imaging (Merkx et al., 2009), or ultrasound (US) (Kok et al., 2015; van Disseldorp et al., 2018) to determine the stresses in the wall of AAAs. Ruptured aneurysms have shown higher peak wall stresses compared to non-ruptured aneurysms (Fillinger et al., 2002). Wall stress analysis either by itself or in combination with other factors (intra-luminal thrombus thickness, relative diameter increase, sex, etc.) has the potential to produce a risk indicator superior to the maximum diameter (Leemans et al., 2017; Maier et al., 2010).

Besides wall stress analysis, mechanical characterization of AAAs has been investigated. Wittek et al. (2013) showed it was

☆ Terms from the medical subject headings (MeSH) list of Index Medicus should be used (see http://www.ncbi.nlm.nih.gov).

* Corresponding author.
E-mail address: n.j.petterson@tue.nl (N.J. Petterson).

https://doi.org/10.1016/j.jbiomech.2019.01.024
0021-9290/

possible to obtain an estimate of the mechanical properties of the abdominal aorta using the 3-D strain field measured with 4-D ultrasound. An iterative inverse method was used where a mechanical model of the aorta is pressurized with an initial guess of material properties, where after the 3-D strain field of the model is compared with that measured by ultrasound. The error between strain fields was used to generate a new guess of material properties. This iterative approach yields subject specific material properties. van Disseldorp et al. (2016a,b) showed this method is also viable by matching displacements rather than strain fields.

Current research on AAA wall stress analysis include the aortic wall and often the intra-luminal thrombus, or post-operative models of stented vessels, while mechanical characterization of the aorta is usually guided by modeling the aorta only (Joldes et al., 2016; Riveros et al., 2015; van Disseldorp et al., 2016a,b). Surrounding tissues are only sparsely used, and efforts found in literature focused on numerical investigation of long term AAA growth (Farsad et al., 2015; Kwon et al., 2015) or the development of a fluid structure interaction methodology (Gasbarro et al., 2007). However, since the spine is located very close to the abdominal aorta, the pulsatile movement of the aortic wall will be confined by the presence of this rigid structure. This will result in an even more inhomogeneous wall motion, which in turn will influence both wall stresses and strains. The aforementioned studies on US-based mechanical characterization use an aorta-only model, without surrounding structures, which may potentially lead to mismatches between the displacement fields simulated and measured.

Hence, this study will investigate the effects of surrounding tissue and spine on the mechanical parameters determined with US-based finite element models of abdominal aortas. Models of increased complexity were created for subject specific aortic geometries in both healthy volunteers and AAA patients and compared to *in vivo* ultrasound motion tracking data. The influence on wall stress, wall strain and estimated shear modulus were examined and compared to conventional (aorta-only) models.

2. Materials and methods

2.1. Population

In this study, 11 healthy volunteers and 7 AAA diagnosed patients were included. Informed consent was given by the subjects prior to inclusion. The local medical ethics committee of the Catharina Hospital Eindhoven approved this study. For volunteer and patient demographics, see Table 1.

2.2. Data acquisition

A Philips iU22 ultrasound scanner equipped with a 3D matrix probe (type:X6-1, center frequency: 3.5 MHz) was used to acquire all ultrasound images (Philips Medical Systems, Bothell, WA, USA). 3D + time images were recorded to assess the motion of the aorta during the cardiac cycle, which resulted of a volume rate of 5–7 Hz. Subjects were lying in supine position and were asked to hold their breath during the acquisition of the images, which took approximately 5 s. The subject's blood pressure in the brachial artery was measured with an arm cuff while in supine position. The brachial pressure is assumed to be equal to the pressure in the abdominal aorta.

Table 1
Subject demographics.

	Volunteers (n = 11)	AAA Patients (n = 7)
Age	21–64	68–81
Gender (M:F)	3:8	7:0
Anterior - posterior diameter	14–24 mm	33–52 mm
Diastolic blood pressure	61–104 mmHg	74–95 mmHg
Systolic blood pressure	105–186 mmHg	118–173 mmHg

2.3. Segmentation

Segmentation of the aortas was done manually in MATLAB (The Mathworks, Natick, MA, USA). First, the aortic wall was segmented in two longitudinal slices located near the maximum diameter of the vessel. These were used to determine the end-diastolic and end-systolic frames of the 4D dataset. Secondly, cross-sectional 2-D images were analyzed slice-by-slice to segment the aorta in the end-diastolic volume frame. These contours were regularized and up-sampled in 3-D to create a smooth surface (van Disseldorp et al., 2016a,b).

2.4. Ultrasound motion tracking

Coarse-to-fine speckle tracking was used to determine 3-D wall displacements from the diastolic to the systolic phase of the cardiac cycle. A two-step correlation approach was used, with an initial kernel size of 1.9 mm × 2.2 mm × 2.3 mm and a search region of 13.1 mm × 11.2 mm × 11.4 mm. The second stage enhanced the accuracy of the first displacement estimate by reducing the search region and kernel size to 5.6 mm × 6.7 mm × 6.8 mm. Median filtering was used to reduce outliers. Finally, the segmented, end-diastolic contours of the aorta were tracked using the frame-to-frame displacement values to determine the end-systolic geometry.

2.5. Mechanical modeling

The aorta geometry obtained from manual segmentation was used to create a 3D mechanical finite element model. The segmented contours served as the inner wall surface of the aorta, which were extended by 3 cm in both proximal and distal direction to prevent boundary effects to influence the FE results within the region of interest (van Disseldorp et al., 2016a,b). The wall volume was created by extruding the inner wall surface in the radial direction by 2 mm. Hence, a constant wall thickness was assumed over the modelled part of the aorta.

The constitutive behavior of the aorta was based on a linearization of a model by Raghavan and Vorp (2000) at the physiological pressure range. Here, the aorta material behavior for this limited strain range was modelled as an incompressible, hyperelastic, neo-Hookean solid (Speelman et al., 2008). The shear modulus of the model was estimated for each subject using an iterative forward finite element approach. In this method, the model is simulated for an initial guess of the shear modulus. Next, the shear modulus is adjusted while minimizing the absolute difference between the modelled displacements and the measured displacements obtained from the 3-D ultrasound data using speckle tracking (van Disseldorp et al., 2016a,b). Since the end-diastolic geometry of the aorta obtained from the 3-D US data was not stress free, the backward incremental method was used to calculate the initial stresses in the wall, present at diastolic blood pressure (de Putter et al., 2007).

Two additional models were created to simulate the tissue surrounding the aorta. An example of the three models for an individual case can be seen in Fig. 1. The first extension was the addition of an abdomen-like block of surrounding soft tissue. The aorta was placed at a depth that is similar to the depth measured in the ultrasound images and an additional 10 cm of surrounding soft tissue was added below the aorta. The block of tissue had the same length as the aorta whereas the width was set at 20 cm (Fig. 1B).

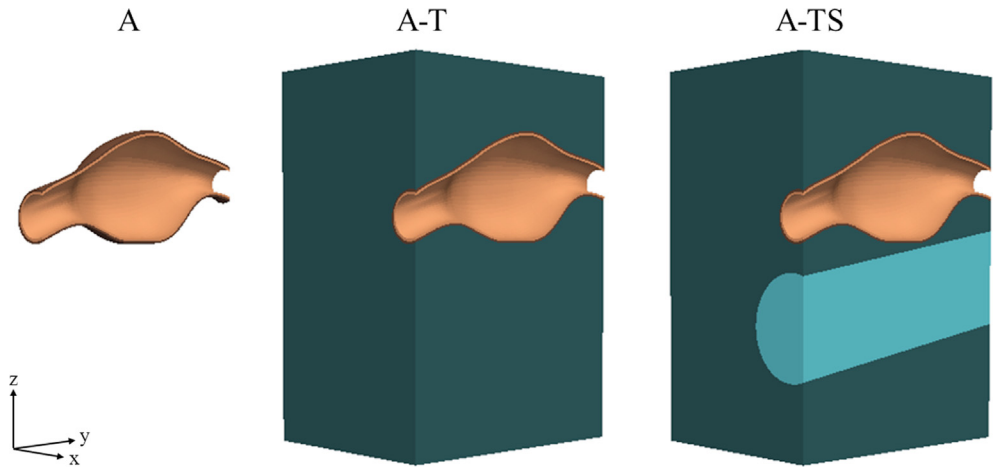

Fig. 1. Finite element mesh geometries of an abdominal aortic aneurysm (A), an aneurysm with surrounding soft tissue (A-T), and an aneurysm, surrounding soft tissue, and the spine (A-TS).

The second extension was the inclusion of a spine model, i.e., a stiff rod simulating the spine. The spine had a diameter of 5 cm and was oriented along the axis of the aorta. Physiologically, the aorta is not located centrally above the spine. CT images showed the center axis of the spine was generally located five mm to the left of the center axis of the aorta and the distance between the aorta and the spine surface was one millimeter. The spine was positioned in the models accordingly.

Mechanical constitutive behavior of both the surrounding soft tissue and the spine was modelled as an incompressible, hyperelastic, neo-Hookean solid with shear modulus of 20 kPa for surrounding soft tissue (Geerligs et al., 2008) and 900 MPa for the spine (Speelman et al., 2008).

Boundary conditions of both displacement and pressure were applied to evaluate the mechanical models. Displacement of the surrounding soft tissue's bottom surface was fixed in all directions as were the front and rear exteriors of the spine. The front and rear ends of the aorta were fixed in the longitudinal direction to prevent elongation while allowing radial motion. For computational stability, the model containing just the aorta had displacements at both ends of the aorta fixed in all directions. The models were inflated from the patient-specific, measured, diastolic to systolic blood pressure to obtain the displacements of the aortic wall.

2.6. Data analysis

Validation of the increasingly complex mechanical models was performed by calculating the mean absolute difference (MAD) of the displacements of the inner aortic wall between ultrasound and mechanical models. This analysis took into account the displacements of the inner wall contours of the aorta in the part that is visible with ultrasound. The improvement in modeling accuracy was quantified by computing the reduction in MAD for each addition to the mechanical model. The aortic motion was chosen as this was the primary target, hence, the motion of the surrounding tissue was not analyzed.

Moreover, Von Mises stresses, shear strains, and aortic shear moduli obtained in the models including the surrounding tissue (A-T) and the spine (A-TS) were compared to the AAA-only model.

3. Results

3.1. Stress

Both peak and 99-percentile Von Mises stresses were higher in patients than in volunteers as expected. Fig. 2 shows however a clear declining trend when the model is extended with surrounding soft tissue. Addition of the soft tissue showed a relative decline in 99-percentile Von Mises stresses of 30 ± 4% and 23 ± 5% in volunteers and patients, respectively. The median Von Mises stresses showed a decrease of 14 ± 6% and 4% ± 4% in volunteers and patients, respectively. The addition of the spine did not show large differences. In Fig. 3 it can be seen that mainly the high peak stresses are decreasing when the model complexity is increased. This showed a more homogeneous stress distribution over the aneurysm wall.

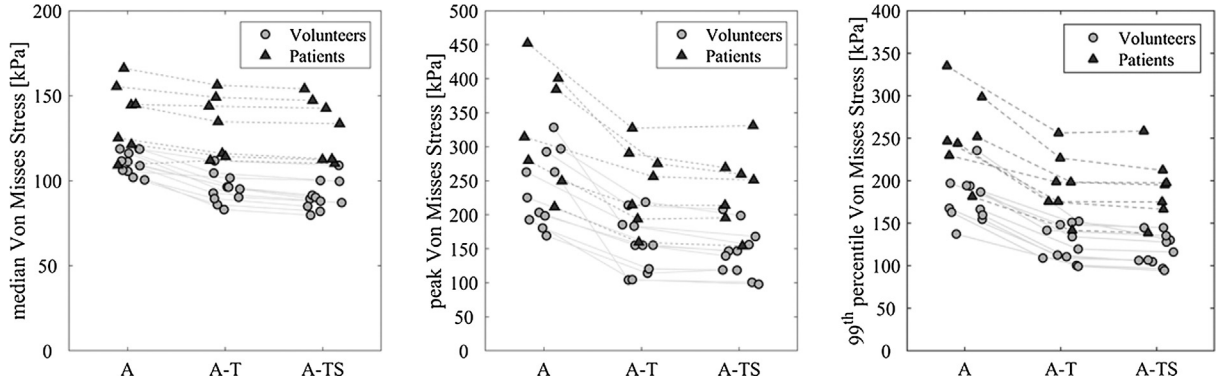

Fig. 2. Stress in the aortic wall in the three complexity models in volunteers and patients. Left: Median Von Mises stress. Middle: Peak Von Mises stress. Right: 99-percentile Von Mises stress.

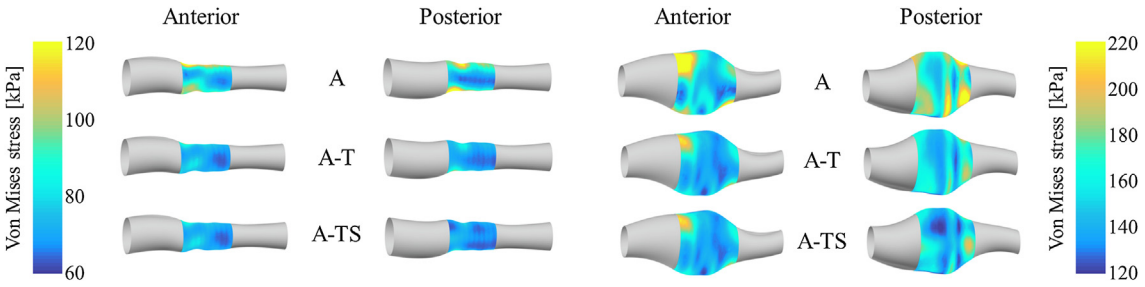

Fig. 3. Von Mises stress distribution in a healthy aorta (left) and an abdominal aortic aneurysm (right) visualized in the anterior and posterior view.

3.2. Moduli

Estimated moduli revealed higher values and a higher variance for patients (694 ± 328 kPa) compared to volunteers (144 ± 61 kPa) as can be seen in Fig. 4. Addition of soft tissue resulted in a decreasing effect on estimated shear modulus, i.e., 20 ± 5% for patients and 12 ± 4% for volunteers. The addition of the spine showed only minor influence on the estimated shear modulus compared to the embedding of the aorta in soft tissue.

3.3. Validation

In Fig. 5 it can be depicted that the displacement of the simple aortic model of both volunteers and AAA patients has a large error on the posterior side, close to the spine. The addition of the soft tissue and especially the spine reduces the posterior displacement errors both in volunteers (0.96 mm to 0.51 mm) and in patients (0.46 mm to 0.38 mm). However, the anterior displacement error in volunteers stays similar (0.53 mm to 0.54 mm), while in patients the anterior displacement error increases (0.40 mm to 0.51 mm). The residual error of all 18 cases between ultrasound and mechanical model displacements are shown in Fig. 6 and clearly reveals a reduction in the axial (z) -displacements when model complexity increases. Fig. 7 shows displacement vectors from both ultrasound displacement tracking and output of the mechanical models in a cross-section of a volunteers aorta. The displacements found in the mechanical model approach the measured displacements the best when both generic surrounding tissue and the spine are included in the model.

3.4. Shear strain

Shear strain in the radial-circumferential direction (ε_{rc}) showed very similar results between the basic aorta model and the more complex surrounding soft tissue model. Shear strain magnitude is 2.0% ± 1.0% (mean ± std) and 0.4% ± 0.2% (mean ± std) for volun-

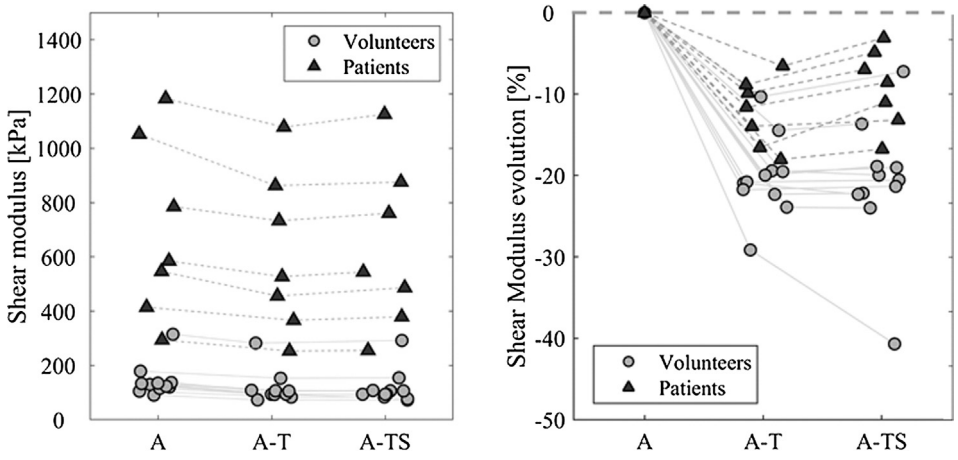

Fig. 4. Evolution of shear modulus in models A-T and A-TS, compared to the standard single aorta model (A).

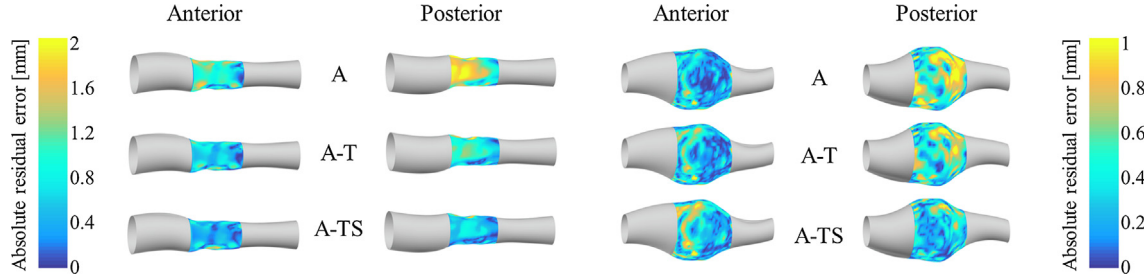

Fig. 5. Absolute error between the displacements found in the mechanical model and those found with ultrasound measurements. Left: anterior and posterior views of a healthy aorta. Right: anterior and posterior views of a AAA.

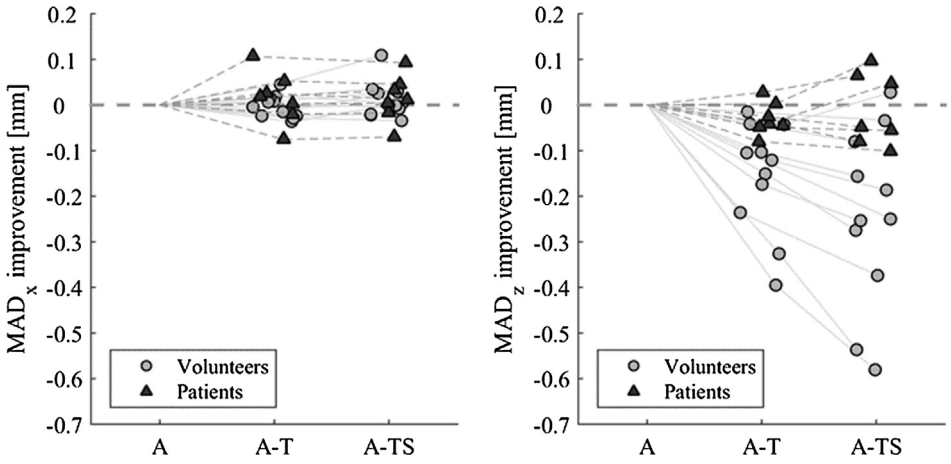

Fig. 6. Mean absolute difference (MAD) improvement of the local displacements between the mechanical model and the ultrasound measurements for all subjects. Left: Displacement improvement in the x direction. Right: Displacement improvement in the z direction.

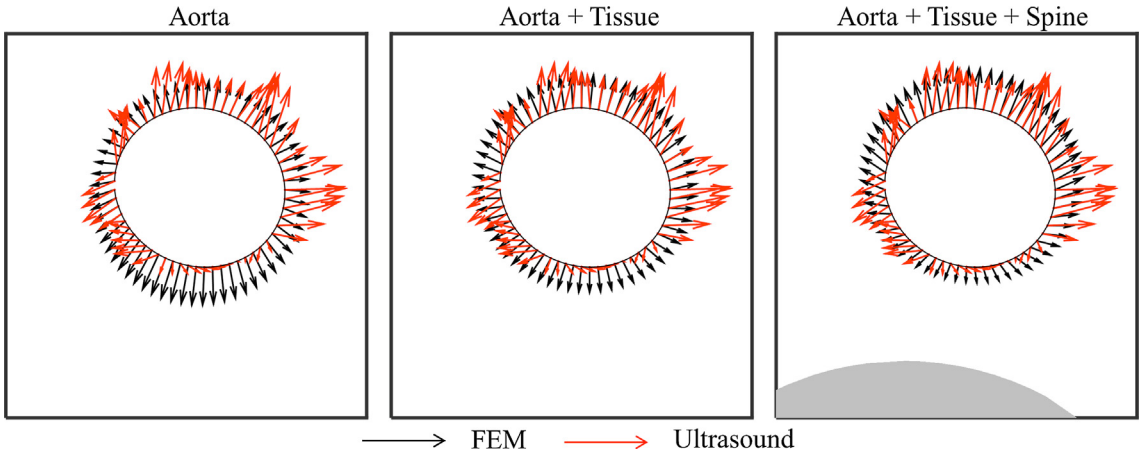

Fig. 7. Displacement vectors of a slice of the aorta. Red arrows: tracking results of ultrasound speckle tracking of the aorta wall; Black arrows: displacements of the aortic wall estimated by the mechanical models. (For interpretation of the references to colour in this figure legend, the reader is referred to the web version of this article.)

teers and patients respectively. The cases without a spine show a very homogeneous strain pattern across the circumference. This is expected since the radial aortic motion is axi-symmetric. However, addition of the spine shows an increase of shear strain around the part located closest to the spine in both volunteers and patients. Fig. 8 shows the magnitude of tissue and spine induced shear strains between the models with added tissue and spine compared to the aorta-only model. The magnitude of spine-induced shear strain lies in the same order of the total shear strain measured in the aorta-only model, namely 2.4% ± 1.1% (mean ± std) and 1.0% ± 0.9% (mean ± std) for volunteers and patients respectively.

4. Discussion

In this study, the influence of surrounding tissues on the estimated wall stress, strain, and shear modulus in mechanical models of the abdominal aorta was investigated.

Results show a large (23–30%) reduction of 99-percentile wall stresses when surrounding tissue is included in the model for both healthy volunteers and AAA patients. The reduction in median wall stresses is minor compared to the decrease in peak and 99-percentile stresses. This indicates a homogenization of wall stress over the entire aorta rather than an overall reduction. Speelman et al. (2010) showed a reduction in 99-percentile wall stresses when including intra-luminal thrombus (ILT). The effects of the ILT are of similar magnitude as the effect of soft tissue inclusion. This implies the importance of both the ILT and soft tissue when performing wall stress analysis.

Estimated shear moduli of the aortic wall were significantly reduced by adding surrounding soft tissue. This is expected from a theoretical point of view, i.e. due to the soft tissue taking up some of the stresses. Therefore, a lower shear modulus with additional surrounding tissue will result in the same displacements measured for the pressure present. This finding emphasizes the difficulty and possible biases involved when estimating mechanical parameters of the vessel as well as the importance of other structures nearby the AAA.

Comparing ultrasound measured displacements with model output reveals an improvement of model accuracy when incorporating both soft tissue and the spine. While a good improvement in the posterior error between model output and measurement data was found in both patients and volunteers, in patients the anterior error increased with addition of surrounding tissues. This might possibly be caused by a low shear modulus of the surrounding tissue, or the omission of the pressure exerted by the probe on

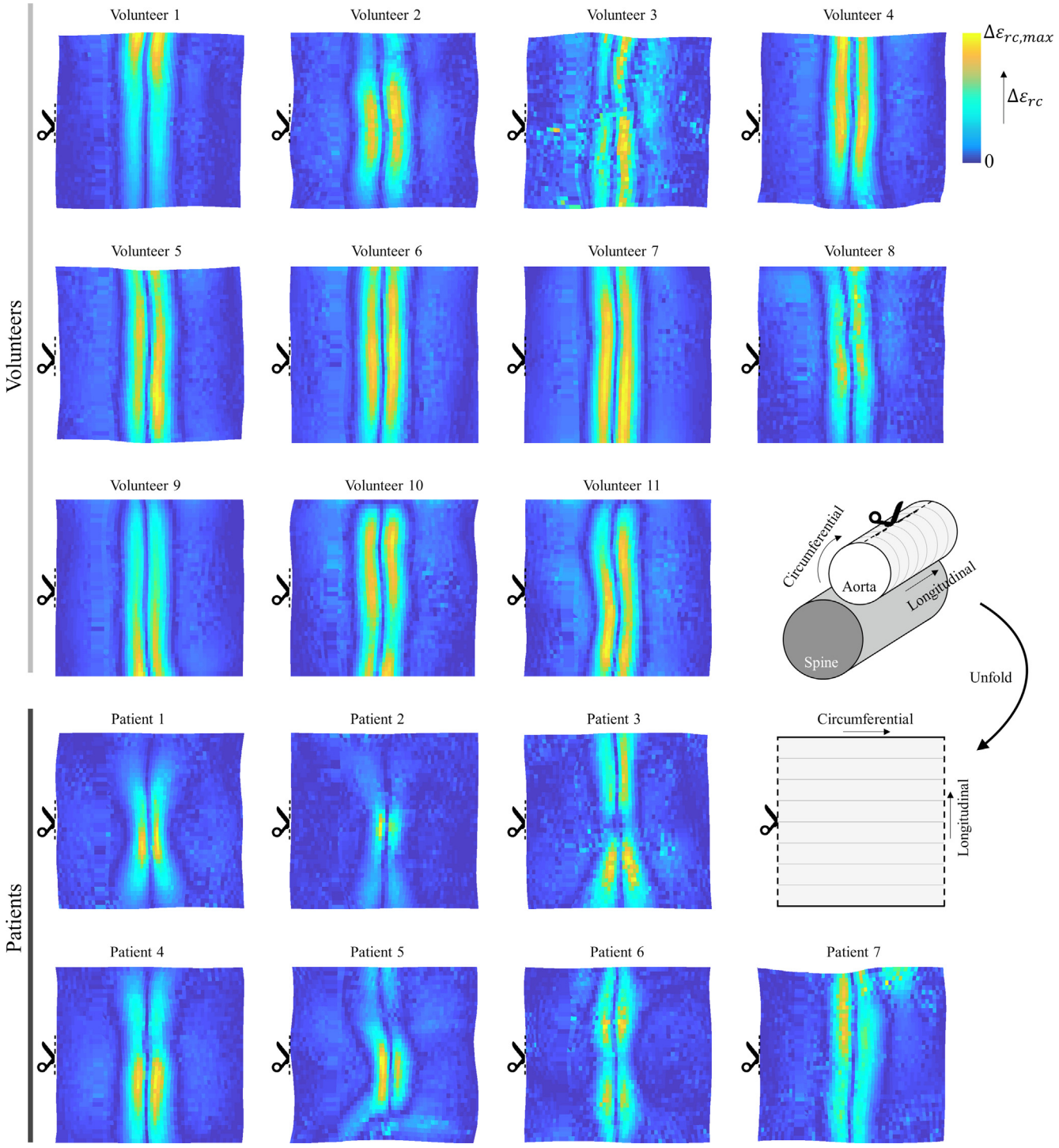

Fig. 8. Shear strains induced by addition the spine (A-TS).

the abdomen in the current modeling framework. These issues require further investigation in future studies. Unfortunately, the displacement measurements of DICOM ultrasound have an anisotropic signal to noise ratio. This makes tracking in the direction perpendicular to the ultrasound propagation direction challenging. Furthermore, stiff aneurysms show minor displacements, which fall close to the DICOM image resolution. These two issues could be solved in the future by using multi-view, raw, radiofrequency ultrasound data.

The introduction of the spine showed a predominant effect on shear strain compared to the other strain directions. Therefore, the strain analysis of this paper focused on radial-circumferential shear strains. Several studies have looked into *in vivo* aortic strain (Brekken et al., 2006; Karatolios et al., 2013; Mix et al., 2017), however no shear strains were reported. Wittek et al. (2013) did report shear strains, yet no link with geometric features surrounding the aorta was made. The demonstrated effect of the spine on shear strain is an interesting finding of this study. Largest changes in

shear strains were found in the posterior side of the aorta, near the spine. A study of Darling et al. (1976) showed that most AAA ruptures occur on the posterior side of the aorta, which is closest to the spine. The elevated levels in shear strain should be further examined to see whether there is a relation between rupture location and elevated shear strain.

One of the major limitations of this study is the low quality aortic wall motion estimation in patients using 4-D ultrasound. The main problem lies with the low amplitude of AAA wall motion, which is not the case in volunteers. Since these vessels are both stiff and dilated, the wall motion decreases towards the image resolution of DICOM ultrasound (~0.5 mm).

Another large drawback of these methods is the low fidelity of surrounding soft tissue characterization. Numerous organs surround the aorta, however, in this study all organs and content in the abdominal cavity were modelled as a continuum, with the exception of the spine. However, it is expected that some structures, e.g. the vena cava and large intestines, will resist motion less than others such as fat. This can influence the outcome of the wall stress analysis. Future work, investigating the differences of a patient-specific cavity model vs. the continuum approach used in this work, needs to be conducted, possibly including the influence of probe pressure.

Moreover, the sensitivity of the biomechanical analysis to the patient-specific spine geometry and location should be quantified. Since the distance of the spine to the aorta is minimal, small variations in spine geometry, e.g. intervertebral discs, can have a large influence on local wall motion, and thus on wall stress. Although ultrasound is not the optimal modality for bone imaging, it can in fact detect the spine surface, which will suffice for this framework as only the interface between the bone and the aorta is of importance. Furthermore, a thrombus can be incorporated in the patients that have an AAA with ILT, this will ensure all possible load-bearing structures present around the abdominal aorta are present in simulations.

In conclusion, this study shows that adding surrounding soft tissue and a spine have a significant effect on AAA rupture-risk related parameter estimates, i.e., peak stress, shear strain, and modulus. Increasing model complexity demonstrates homogenization of wall stresses, reduction in homogeneity of shear strain, and a decrease in estimated aortic wall shear modulus.

Conflict of interest

None.

Acknowledgements

This study was funded by an unrestricted educational grant of the Lijf & Leven foundation and IMPULS-II.

References

Brekken, R., Bang, J., Ødegård, A., Aasland, J., Hernes, T.A.N., Myhre, H.O., 2006. Strain estimation in abdominal aortic aneurysms from 2-D ultrasound. Ultrasound Med. Biol. 32, 33–42. https://doi.org/10.1016/j.ultrasmedbio.2005.09.007.

Darling, R.C., Messina, C.R., Brewster, D.C., Ottinger, L.W., 1976. Autopsy study of unoperated abdominal aortic aneurysms. Cardiovasc. Surg. 56, 4.

de Putter, S., Wolters, B.J.B.M., Rutten, M.C.M., Breeuwer, M., Gerritsen, F.A., van de Vosse, F.N., 2007. Patient-specific initial wall stress in abdominal aortic aneurysms with a backward incremental method. J. Biomech. 40, 1081–1090. https://doi.org/10.1016/j.jbiomech.2006.04.019.

Erhart, P., Hyhlik-Dürr, A., Geisbüsch, P., Kotelis, D., Müller-Eschner, M., Gasser, T.C., von Tengg-Kobligk, H., Böckler, D., 2015. Finite element analysis in asymptomatic, symptomatic, and ruptured abdominal aortic aneurysms. in search of new rupture risk predictors. Eur. J. Vasc. Endovasc. Surg. 49, 239–245. https://doi.org/10.1016/j.ejvs.2014.11.010.

Farsad, M., Zeinali-Davarani, S., Choi, J., Baek, S., 2015. Computational growth and remodeling of abdominal aortic aneurysms constrained by the spine. J. Biomech. Eng. 137. https://doi.org/10.1115/1.4031019. 091008 091008.

Fillinger, M.F., Marra, S.P., Raghavan, M.L., Kennedy, F.E., 2003. Prediction of rupture risk in abdominal aortic aneurysm during observation: Wall stress versus diameter. J. Vasc. Surg. 37, 724–732. https://doi.org/10.1067/mva.2003.213.

Fillinger, M.F., Raghavan, M.L., Marra, S.P., Cronenwett, J.L., Kennedy, F.E., 2002. In vivo analysis of mechanical wall stress and abdominal aortic aneurysm rupture risk. J. Vasc. Surg. 36, 589–597. https://doi.org/10.1067/mva.2002.125478.

Gasbarro, M.D., Shimada, K., Martino, E.S.D., 2007. Mechanics of abdominal aortic aneurysm. Eur. J. Comput. Mech. 16, 337–363. https://doi.org/10.3166/remn.16.337-363.

Gasser, T.C., 2016. Biomechanical rupture risk assessment. AORTA J. 4, 42–60 https://doi.org/10.12945/j.aorta.2015.15.030.

Geerligs, M., Peters, G.W.M., Ackermans, P.A.J., Oomens, C.W.J., Baaijens, F.P.T., 2008. Linear viscoelastic behavior of subcutaneous adipose tissue. Biorheology 45, 677–688. https://doi.org/10.3233/BIR-2008-0517.

Indrakusuma, R., Jalalzadeh, H., Planken, R.N., Marquering, H.A., Legemate, D.A., Koelemay, M.J.W., Balm, R., 2016. Biomechanical imaging markers as predictors of abdominal aortic aneurysm growth or rupture: a systematic review. Eur. J. Vasc. Endovasc. Surg. 52, 475–486. https://doi.org/10.1016/j.ejvs.2016.07.003.

Joldes, G.R., Miller, K., Wittek, A., Doyle, B., 2016. A simple, effective and clinically applicable method to compute abdominal aortic aneurysm wall stress. J. Mech. Behav. Biomed. Mater. Special issue: Mechanics of biological membranes 58, 139–148. https://doi.org/10.1016/j.jmbbm.2015.07.029.

Karatolios, K., Wittek, A., Nwe, T.H., Bihari, P., Shelke, A., Josef, D., Schmitz-Rixen, T., Geks, J., Maisch, B., Blase, C., Moosdorf, R., Vogt, S., 2013. Method for aortic wall strain measurement with three-dimensional ultrasound speckle tracking and fitted finite element analysis. Ann. Thorac. Surg. 96, 1664–1671. https://doi.org/10.1016/j.athoracsur.2013.06.037.

Kok, A.M., Nguyen, V.L., Speelman, L., Brands, P.J., Schurink, G.-W.H., van de Vosse, F.N., Lopata, R.G.P., 2015. Feasibility of wall stress analysis of abdominal aortic aneurysms using three-dimensional ultrasound. J. Vasc. Surg. 61, 1175–1184. https://doi.org/10.1016/j.jvs.2014.12.043.

Kwon, S.T., Burek, W., Dupay, A.C., Farsad, M., Baek, S., Park, E.-A., Lee, W., 2015. Interaction of expanding abdominal aortic aneurysm with surrounding tissue: retrospective CT image studies. J. Nat. Sci. 1, e150.

Leemans, E.L., Willems, T.P., van der Laan, M.J., Slump, C.H., Zeebregts, C.J., 2017. Biomechanical indices for rupture risk estimation in abdominal aortic aneurysms biomechanical indices for rupture risk estimation in abdominal aortic aneurysms. J. Endovasc. Ther. 24, 254–261. https://doi.org/10.1177/1526602816680088.

Maier, A., Gee, M.W., Reeps, C., Pongratz, J., Eckstein, H.-H., Wall, W.A., 2010. A comparison of diameter, wall stress, and rupture potential index for abdominal aortic aneurysm rupture risk prediction. Ann. Biomed. Eng. 38, 3124–3134. https://doi.org/10.1007/s10439-010-0067-6.

Merkx, M.A.G., van 't Veer, M., Speelman, L., Breeuwer, M., Buth, J., van de Vosse, F.N., 2009. Importance of initial stress for abdominal aortic aneurysm wall motion: dynamic MRI validated finite element analysis. J. Biomech. 42, 2369–2373. https://doi.org/10.1016/j.jbiomech.2009.06.053.

Mix, D.S., Yang, L., Johnson, C.C., Couper, N., Zarras, B., Arabadjis, I., Trakimas, L.E., Stoner, M.C., Day, S.W., Richards, M.S., 2017. Detecting regional stiffness changes in aortic aneurysmal geometries using pressure-normalized strain. Ultrasound Med. Biol. 43, 2372–2394. https://doi.org/10.1016/j.ultrasmedbio.2017.06.002.

Moll, F.L., Powell, J.T., Fraedrich, G., Verzini, F., Haulon, S., Waltham, M., van Herwaarden, J.A., Holt, P.J.E., van Keulen, J.W., Rantner, B., Schlösser, F.J.V., Setacci, F., Ricco, J.-B., 2011. Management of abdominal aortic aneurysms clinical practice guidelines of the european society for vascular surgery. Eur. J. Vasc. Endovasc. Surg. Manage. Abdominal Aortic Aneurysms Clinical Practice Guidelines European Soc. Vascular Surgery 41, S1–S58. https://doi.org/10.1016/j.ejvs.2010.09.011.

Nicholls, S.C., Gardner, J.B., Meissner, M.H., Johansen, K.H., 1998. Rupture in small abdominal aortic aneurysms. J. Vasc. Surg. 28, 884–888. https://doi.org/10.1016/S0741-5214(98)70065-5.

Riveros, F., Martufi, G., Gasser, T.C., Rodriguez-Matas, J.F., 2015. On the Impact of Intraluminal Thrombus Mechanical Behavior in AAA Passive Mechanics. Ann. Biomed. Eng. 43, 2253–2264. https://doi.org/10.1007/s10439-015-1267-x.

Raghavan, M.L., Vorp, D.A., 2000. Toward a biomechanical tool to evaluate rupture potential of abdominal aortic aneurysm: identification of a finite strain constitutive model and evaluation of its applicability. J. Biomech. 33, 475–482. https://doi.org/10.1016/S0021-9290(99)00201-8.

Speelman, L., Bosboom, E.M.H., Schurink, G.W.H., Hellenthal, F.A.M.V.I., Buth, J., Breeuwer, M., Jacobs, M.J., van de Vosse, F.N., 2008. Patient-specific AAA wall stress analysis: 99-percentile versus peak stress. Eur. J. Vasc. Endovasc. Surg. Off. J. Eur. Soc. Vasc. Surg. 36, 668–676. https://doi.org/10.1016/j.ejvs.2008.09.007.

Speelman, L., Schurink, G.W.H., Bosboom, E.M.H., Buth, J., Breeuwer, M., van de Vosse, F.N., Jacobs, M.H., 2010. The mechanical role of thrombus on the growth rate of an abdominal aortic aneurysm. J. Vasc. Surg. 51, 19–26. https://doi.org/10.1016/j.jvs.2009.08.075.

The UK Small Aneurysm Trial Participants, 1998. Mortality results for randomised controlled trial of early elective surgery or ultrasonographic surveillance for small abdominal aortic aneurysms. The Lancet 352, 1649–1655. https://doi.org/10.1016/S0140-6736(98)10137-X.

van Disseldorp, Emiel M.J., Hobelman, K.H., Petterson, N.J., van de Vosse, F.N., van Sambeek, M.R.H.M., Lopata, R.G.P., 2016a. Influence of limited field-of-view on wall stress analysis in abdominal aortic aneurysms. J. Biomech. Cardiovascular Biomech. Health Dis. 49, 2405–2412. https://doi.org/10.1016/j.jbiomech.2016.01.020.

van Disseldorp, E.M.J., Petterson, N.J., Rutten, M.C.M., van de Vosse, F.N., van Sambeek, M.R.H.M., Lopata, R.G.P., 2016b. Patient specific wall stress analysis and mechanical characterization of abdominal aortic aneurysms using 4D ultrasound. Eur. J. Vasc. Endovasc. Surg. 52, 635–642. https://doi.org/10.1016/j.ejvs.2016.07.088.

Van Disseldorp, E.M.J., Petterson, N.J., van de Vosse, F.N., van Sambeek, M.R.H.M., Lopata, R.G.P., 2018. Quantification of aortic stiffness and wall stress in healthy volunteers and abdominal aortic aneurysm patients using time-resolved 3D ultrasound: a comparison study. Heart J. Cardiovasc. Imaging Eur. https://doi.org/10.1093/ehjci/jey051.

Wittek, A., Karatolios, K., Bihari, P., Schmitz-Rixen, T., Moosdorf, R., Vogt, S., Blase, C., 2013. In vivo determination of elastic properties of the human aorta based on 4D ultrasound data. J. Mech. Behav. Biomed. Mater. 27, 167–183. https://doi.org/10.1016/j.jmbbm.2013.03.014.